IL NUOVO CIMENTO **41 C** (2018) 104
DOI 10.1393/ncc/i2018-18104-x

COMMUNICATIONS: SIF Congress 2017

The glass transition in colloidal suspensions of silica nanoparticles in a water-lutidine mixture: A photon correlation study

A. MARTINELLI([1]) on behalf of F. DALLARI([1]), G. GRÜBEL([2]), F. ZONTONE([3]) and G. MONACO([1])

([1]) *Department of Physics, University of Trento - Trento, Italy*
([2]) *Department of Physics, University of Hamburg - Hamburg, Germany*
([3]) *European Synchrotron Radiation Facility - Grenoble, France*

received 30 January 2018

Summary. — We discuss the structural and dynamical properties of a colloidal glass of silica nanoparticles in a water-lutidine mixture probed using photon correlation techniques. We describe the small angle set-up used to perform X-ray photon correlation spectroscopy (XPCS) experiments and the procedure followed to measure the volume fraction of the sample. We describe the structure of the glass using a short range potential model and a theoretical structure factor within the mean spherical approximation. The dynamics finally is characterized by a Gaussian-like intermediate scattering function which is not compatible with the classical picture of an heterogeneous diffusive process.

1. – Introduction

Colloidal systems have been investigated deeply in the last few decades. Nowadays nanoparticles (NP) are arousing interest due to the wealth of possibilities that they are manifesting. Gold and synthetic NP for gene and drug delivery, noble metals NP functionalized with DNA to build complex nanostructures, quantum dots and catalists are only few examples [1-3].

In this article we discuss the structural and dynamical properties of a concentrated suspension (volume fraction $\phi = (42 \pm 2)\%$) of silica nanoparticles in a water-2,6 lutidine ($(CH_3)_3C_5H_3N$) mixture (0.25 lutidine mass fraction). The water-lutidine solution has a coexistence curve of the two liquid phases with a lower critical point near the mass fraction ~ 0.3 of lutidine in water and a critical temperature of 34 °C [4]. This binary mixture exhibits an uncommon feature when it is placed in contact with silica surfaces: a so-called wetting transition takes place, that is the lutidine separates from water and covers silica surfaces with a layer thickness that depends on the temperature of the system [5]. This layer weakens the repulsive electrostatic interaction between the colloids

and induces aggregation in diluted solutions of silica nanoparticles in near critical water-lutidine mixtures [6, 7].

It was observed using photon correlation techniques that high volume fraction suspensions do not show a temperature induced aggregation but a glass-glass transition between a repulsive and an attractive glass [8].

We report here a detailed study of a colloidal repulsive glass of 100 nm diameter SiO_2 particles in a water-2,6 lutidine mixture (0.25 lutidine mass fraction) at the packing fraction $\phi = (42 \pm 2)\%$ and at the temperature $T = (32.00 \pm 0.01)\,^{\circ}\mathrm{C}$.

2. – Experimental details

2˙1. *Photon correlation.* – Photon correlation is a well-known technique [9]. In the so-called homodyne configuration one performs the autocorrelation of the scattered intensity at a given scattering vector q:

$$g_2(q,\tau) := \frac{\langle I(q,t)I(q,t+\tau)\rangle_t}{\langle I(q,t)\rangle_t^{\,2}} = 1 + \alpha|F(q,\tau)|^2, \tag{1}$$

where $\langle ...\rangle_t$ is a temporal average, α is the contrast and $F(q,\tau)$ is the intermediate scattering function. The last equality is known as the Siegert relation, valid in the Gaussian approximation [9]. Since the intermediate scattering function is the Fourier transform of the Van-Hove self–space-time correlation function, a photon correlation experiment gives direct information on the dynamical properties. In most of the cases, the intermediate scattering function can be modelled as a modified exponential function (KWW function) [10]:

$$F(q,\tau) \propto e^{(-\Gamma\tau)^{\beta}}, \tag{2}$$

where β is known as stretching parameter and Γ^{-1} is the decay time.

It is clear that in order to obtain a reliable autocorrelation function, one needs to integrate for a time much longer than the typical decorrelation time of the intermediate scattering function. However, in glassy-like systems this time could exceed hundreds of seconds, causing difficulties in the use of this technique. To overcome the related statistical limitations the so-called multispeckle approach has been developed [11]. With the use of a 2D detector, one can perform an average over the pixels related to the same exchanged wave vector q, reducing the needed integration time of a factor equal to the number of speckles which are taken into the average.

2˙2. *Experimental set-up.* – We carried out an X-Ray photon correlation experiment in small angle geometry (XPCS-SAXS) at the coherent station of the ID10 beamline at the European Synchrotron Radiation Facility (ESRF) in Grenoble (France).

Synchrotrons are basically incoherent sources of X-rays. The way to get a partially coherent beam is to use slits, pinholes and monochromators. Indeed transverse and longitudinal coherence lengths at a distance R from the source can be defined as [12]:

$$\xi_t \simeq \frac{\lambda R}{2\Sigma}, \quad \xi_l \simeq \frac{\lambda^2}{\Delta\lambda}, \tag{3}$$

where λ and $\frac{\Delta\lambda}{\lambda}$ are, respectively, the wavelength and the relative bandwidth of the beam and Σ is the source size.

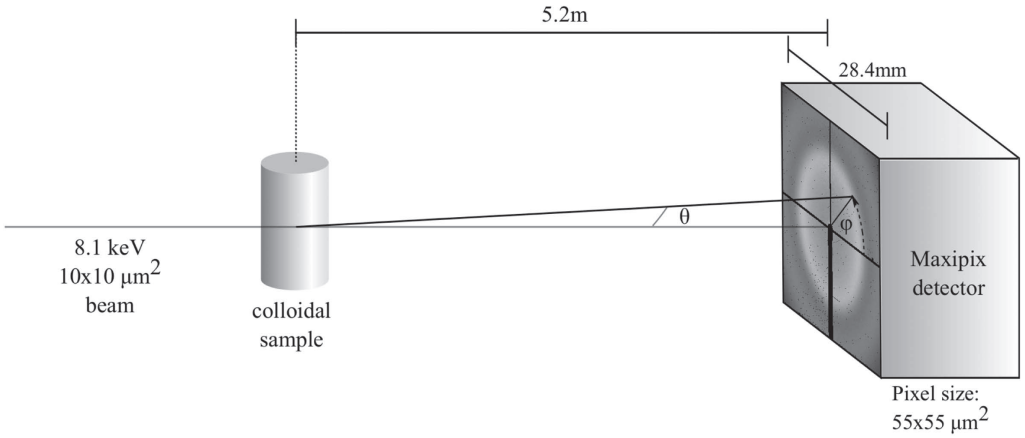

Fig. 1. – Scheme of the experimental set-up for small angle coherent X-ray scattering. The scattered intensity is collected with the Maxipix (2D single-photon counterdetector) [14].

With a Si(111) monochromator one is able to achieve an energy resolution $\frac{\Delta\lambda}{\lambda} = 1.4\times10^{-4}$, which corresponds to $\xi_l \simeq 1\,\mu$m at $E = 8.1\,$keV. With regard to the transverse coherence, at a given energy the decisive factor is the ratio $\frac{R}{\Sigma}$. For this reason, the sample is kept far ($R \sim 50\,$m) from the source and with a combination of lenses and slits a coherent beam of $10 \times 10\,\mu$m^2 size is obtained [13].

In fig. 1 the scheme of the experimental set-up is reported. In order to perform a coherent scattering experiment the sample volume must be illuminated coherently. For this reason, the path-length difference (PLD) for rays in the scattering volume cannot exceed the longitudinal coherence ξ_l. The PLD can be written as [12]

$$\text{PLD} \simeq 2W \sin^2 \frac{\theta}{2} + d \sin\theta, \tag{4}$$

where W is the thickness of the sample, θ is the scattering angle as reported in fig. 1 and d is the beam diameter. A sample thickness $W = 500\,\mu$m was chosen for the experiment, which fulfils the requirements of eq. (4) for the whole detector surface.

It can be shown [9] that the maximum contrast in the autocorrelation function is achieved when at most one speckle impinges on the detector. Since the multispeckle technique is used to increase the statistical accuracy, the best performance is obtained with speckles of the same size as the pixel ($55 \times 55\,\mu$m^2). The speckle linear size can be estimated as

$$l_c \sim \frac{\lambda}{\Omega} \simeq \frac{1.22 \cdot \lambda D}{d}, \tag{5}$$

where λ is the wavelength of the incident beam, Ω is the angle of the source subtended at the detector, D is the source-detector distance, d is the beam diameter and the term 1.22 is introduced to take into account the cylindrical symmetry of the scattering volume. A distance $D = (5.22 \pm 0.01)\,$m was used in the experiment, which implies speckles with a linear size of $\sim 100\,\mu$m.

2˙3. *Sample preparation.* – The samples were prepared from a diluted suspension of silica Sicastar®(Micromod) nanoparticles (100 nm diameter, mass concentration 100 mg/mL of solution). The right amount of 2,6-lutidine (Sigma-Aldrich®) was added to the solution to reach a lutidine-water mass fraction $C_{lw} = 0.25$. The obtained suspension was then centrifuged and the exceeding solvent removed to obtain the desired volume fraction of silica with respect to the solution. The sample was then shaken on a vortex mixer to get a homogeneous suspension and filled into Mark-tubes capillaries made of borosilicate glass (Hilgenberg®) of outer diameter 0.5 mm and wall thickness 0.01 mm and placed in a ultrasonic bath for 1 minute to remove air bubbles.

3. – Measuring the volume fraction

In order to obtain high volume fractions ($\phi \sim 40\%$) most of the solvent has to be removed. Since the particles diffuse into the solution after centrifugation, it is difficult to estimate the exact final volume fraction of the colloidal system. It is then worth to perform a direct measurement of the volume fraction.

The transmitted part of an X-ray beam through a sample of thickness x can be modelled as [15]

$$I = T \cdot I_0 = I_0 e^{-\mu x}, \tag{6}$$

where I and I_0 are, respectively, the transmitted and incident beams, T is the transmission coefficient and μ is the attenuation coefficient of the sample. In the case of a colloidal suspension, one can model it with $\mu = (1-\phi)\mu_s + \phi\mu_p$, where ϕ is the volume fraction, μ_s is the attenuation coefficient of the solvent and μ_p is the one relative to the particles. To take into account the thickness of the walls of the capillary, the transmission coefficient T is divided by the one obtained for an empty borosilicate capillary ($T_{empty} = 0.83 \pm 0.02$). Finally, the volume fraction can be calculated as

$$\phi = \frac{-\log(\frac{T}{T_{empty}})\frac{1}{\xi} - (C_L \cdot \mu_L + (1 - C_L) \cdot \mu_W)}{\mu_{SiO_2} - (C_L \cdot \mu_L + (1 - C_L) \cdot \mu_W)}, \tag{7}$$

where C_L is the mass fraction of lutidine in the solvent, μ_L and μ_W are the absorption coefficients for lutidine and water, respectively, and ξ is the inner diameter of the capillary.

An intensity profile (fig. 2) is obtained scanning the sample across the beam while measuring the intensity on the 2D detector. The points outer of the capillary are fitted with a linear law while the bottom of the capillary is fitted with a third power polynomial function.

4. – Structural properties

The experimental scattered intensity is extracted from the images with the following procedure. For each image, dead pixels are masked and the intensity integrated azimuthally (φ) over rings of width Δr centred on the transmitted beam (fig. 1). Then 100 of these spectra (corrected for the subtended solid angle) are averaged to get a standard deviation for each point $I(q)$.

In the kinetic approximation the scattered intensity is

$$I(\vec{q}) \propto |f(\vec{q})|^2 S(\vec{q}), \tag{8}$$

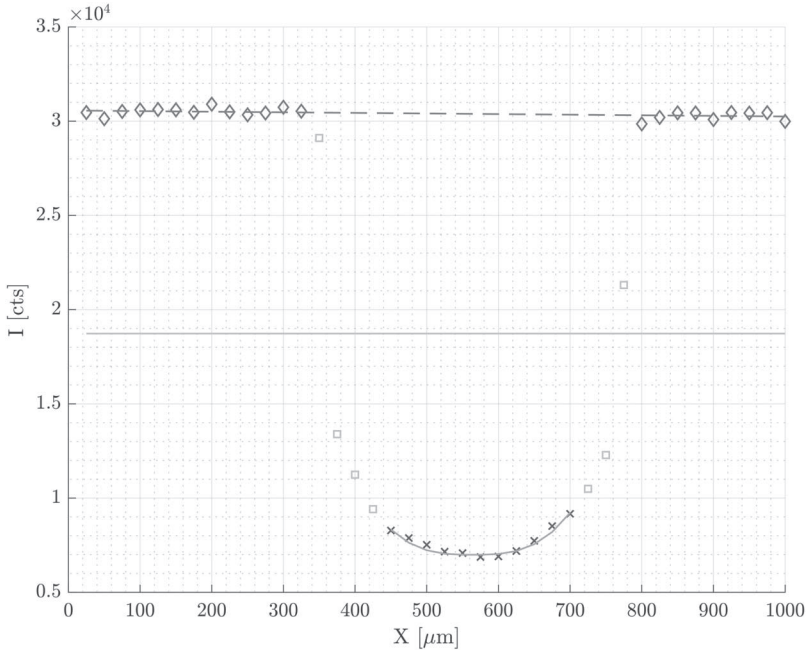

Fig. 2. – Example of intensity profile obtained for a volume fraction of $\phi = (42 \pm 2)\%$. To get a reliable value of I_0 the data corresponding to the transmission out of the sample ($\diamond$) are fitted with a linear law; those corresponding to the bottom of the capillary ($\times$) are fitted with a third power polynomial function. To get a correct estimate of the diameter of the capillary, the half-maximum width is extracted using a linear interpolation.

where $|f(\vec{q})|^2$ is the form factor and $S(\vec{q})$ is the structure factor.

4˙1. *Form factor*. – The form factor $|f(\vec{q})|^2$ is nothing but the Fourier transform of the charge density. In the case of colloidal suspensions the form factor is described in terms of the relative density $\rho = \rho_p - \rho_s$, where ρ_p is the charge density of the suspended particles and ρ_s is the charge density of the solvent.

The form factor of a sphere is [16]

$$|f(|\vec{q}|)|^2 = \left| \rho \frac{4}{3} \pi R^3 \frac{[\sin(qR) - qR\cos(qR)]}{(qR)^3} \right|^2, \tag{9}$$

where R is the radius of the sphere and q the exchanged wave vector. It is important to stress the fact that for symmetry reasons, $|f(\vec{q})|^2 = |f(|\vec{q}|)|^2$.

Since the particles are not monodispersed one has to consider the contribution in the form factor due to different particle's radii. The particle size distribution is modelled with the Schultz distribution

$$f_z(R) = \frac{1}{z!}[z + 1/\bar{r}]^{z+1} r^z \exp -(z+1)r/\bar{r} \tag{10}$$

with $\bar{r}$ the average particle radius and z a parameter that is related to the second moment of the distribution, *i.e.* $\langle R^2 \rangle - \langle R \rangle^2 = \bar{r}^2/(z+1)$. For this particular distribution an

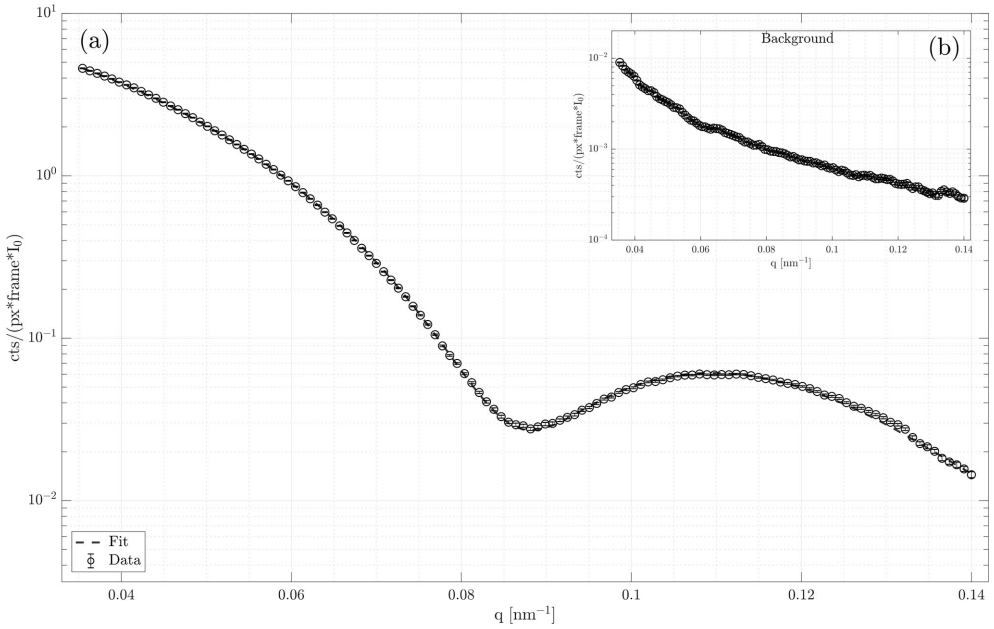

Fig. 3. – (a) Experimental form factor after background subtraction (∘) and best fit (dashed line) performed using a Levenberg-Marquardt nonlinear least-squares algorithm. The obtained parameters are $\langle R\rangle = (51 \pm 1)$ nm and $\sqrt{\langle R^2\rangle - \langle R\rangle^2}/\langle R\rangle = (8 \pm 1)\%$ (b) Background measured with a capillary and the solvent.

analytic function exists to model the form factor [17].

In fig. 3 the experimental form factor is reported after background subtraction. The fitting function is the form factor for polydispersed spheres convoluted with the width of the rings used for the calculation of the experimental intensity.

4˙2. *Structure factor*. – The structure factor is strictly related to the correlation function between particles. Indeed it comes out in the scattered intensity as the interference of the scattered field from different particles. Thanks to this, one can recover structural information such as the pair correlation function ($g(r)$) and the interaction potential. A complete treatment can be found in dedicated books [18] and here only few fundamental results are reported.

The structure factor for an isotropic homogeneous system can be written as

$$S(q) - 1 = n_0 \int \mathrm{d}r 4\pi r^2 \frac{\sin qr}{qr} \left[h(r)\right] \tag{11}$$

with n_0 the average particle density and $h(r)$ the total correlation function function defined as $g(r) - 1$. The Ornstein-Zernike equation [19] expresses the total correlation function in terms of the direct correlation function $\hat{c}(q)$:

$$\hat{h}(q) = \frac{\hat{c}(q)}{1 - \rho\hat{c}(q)}. \tag{12}$$

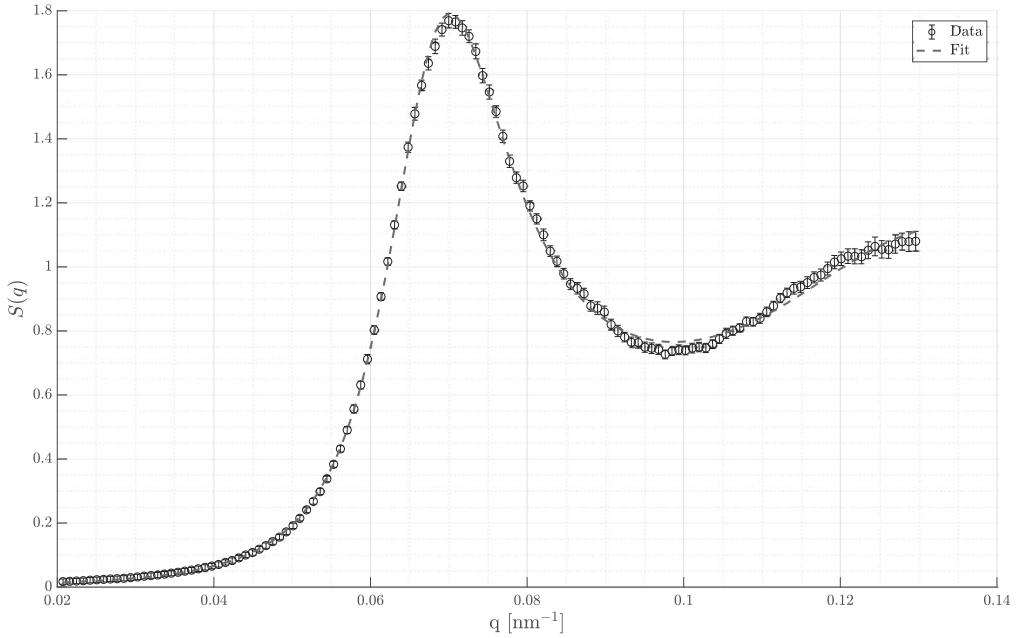

Fig. 4. – Experimental structure factor (∘) and the best fit (dashed line) with eq. (14).

The function $\hat{c}(q)$ is the correlation between particles 1 and 2 only due to the direct interaction between the two particles. Following the idea of the DLVO theory [20,21], the interaction potential between the colloids is modelled with a long-range van der Waals attraction (neglected in the present case) and a short-range electrostatic repulsion:

$$U(r) = \begin{cases} \infty, & \text{if } r < \sigma, \\ \pi\epsilon_0\epsilon\,\sigma^2{\Psi_0}^2\dfrac{e^{-k(r-\sigma)}}{r}, & \text{if } r > \sigma, \end{cases} \tag{13}$$

with σ the diameter of the particles, r the relative distance, Ψ_0 the surface potential and k the inverse of the screening length.

It is possible to solve analytically eq. (12) within the mean spherical approximation [22,23]:

$$\begin{cases} h(x) = -1, & \text{if } x < 1, \\ c(x) = -\beta U(x) = -\gamma\dfrac{e^{-k'x}}{x}, & \text{if } x > 1, \end{cases} \tag{14}$$

where $x = r/\sigma$ and $\gamma = \beta\pi\epsilon\epsilon_0\sigma{\Psi_0}^2 e^k$ with β the Boltzmann factor $1/k_BT$. The total dielectric constant ϵ is calculated linearly combining the ones relative to water and lutidine.

In fig. 4 the experimental structure factor is reported together with the best fit. The parameters of the fitting function [23] are the volume fraction ϕ, the inverse of the reduced screening length $k' = k\sigma$ and the surface potential Ψ_0. The obtained parameters

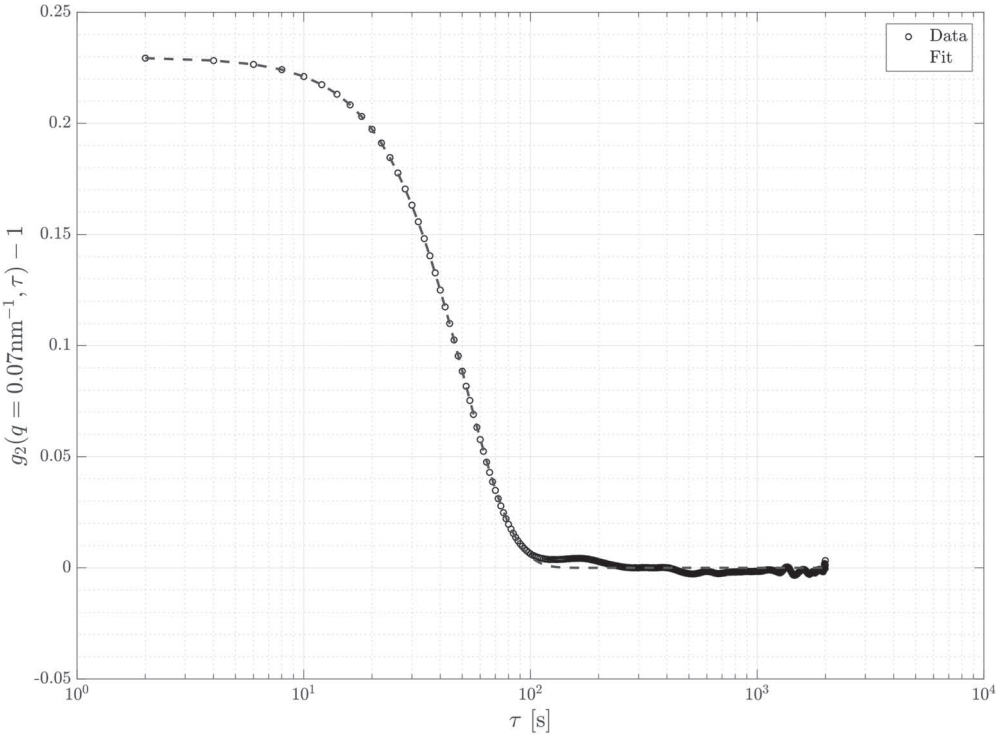

Fig. 5. – Autocorrelation function (∘) calculated on the peak of the structure factor ($q = 0.07\,\text{nm}^{-1}$) and the best fit (dashed line) using eq. (1) and eq. (2). The obtained parameters are $\Gamma^{-1} = (72 \pm 1)\,\text{s}$ and $\beta = (2.0 \pm 0.1)$.

with a non-linear fit (Levenberg-Marquardt least-squares algorithm) are $k' = 2.5 \pm 0.1$, $\Psi_0 = (15.7 \pm 0.5)\,\text{mV}$ and $\phi = 0.41 \pm 0.01$. This last value is in agreement with the one obtained with the transmission measurements ($\phi = 0.42 \pm 0.02$).

5. – Dynamical properties

It is well established that near the glass transition the stretching parameter (β) of the KWW function is usually smaller than 1. This behaviour is attributed to a distribution of simple exponential relaxation processes [24, 25].

In fig. 5 the autocorrelation function is reported, calculated at the peak of the structure factor ($q = 0.07\,\text{nm}^{-1}$) with the multispeckle approach. The value obtained from the fit for the stretching parameter is $\beta = (2.0 \pm 0.1)$. A compressed ($\beta > 1$) behaviour cannot be explained with a superposition of simple exponentials. This peculiar decay is observed in colloidal systems [26] and in metal glasses [27] where it is attributed to the presence of internal stresses. Simulations on colloidal gels have recently shown that the intermittent microscopic dynamics (rearrangement of the gel connections) leads to a faster than exponential relaxation process and a super-diffusive particle dynamics [28,29]. A clear understanding of this phenomenon remains however a topic of current research.

6. – Conclusions

We have characterized a colloidal glass of silica nanoparticles in a water-lutidine bynary mixture. We have modelled the interaction potential with a short-range screened Coulombic repulsion. The calculated structure factor in the mean spherical approximation is in agreement with the experimental data. From a dynamical point of view, we have observed a compressed behaviour of the intermediate scattering function. Despite this feature is common in soft matter systems, the process beyond it is still argument of debate and it is not fully clarified.

* * *

We acknowledge the European Synchrotron Radiation Facility for provision of synchrotron radiation facilities, in particular we thank Karim Lhoste for the technical support and Diego Pontoni for the assistance in using the Soft Matter Laboratory of PSCM.

REFERENCES

[1] Samanta A. and Medintz I. L., *Nanoscale*, **8** (2016) 9037.
[2] Nozik A. J., Beard M. C., Luther J. M., Law M., Ellingson R. J. and Johnson J. C., *Chem. Rev.*, **110** (2010) 6873.
[3] Turner M., Golovko V., Vaughan O., Abdulkin P., Berenguer-Murcia A., Tikhov M., Johnson B. and Lambert R., *Nature*, **454** (2008) 981.
[4] Handschy M. A., Mockler R. C. and O'Sullivan W. J., *Chem. Phys. Lett.*, **76** (1980) 172.
[5] Beysens D. and Estéve D., *Phys. Rev. Lett.*, **54** (1985) 2123.
[6] Beysens D. and Narayanan T., *J. Stat. Phys.*, **95** (1999) 997.
[7] Pontoni D., Narayanan T., Petit J.-M., Grbel G. and Beysens D., *Phys. Rev. Lett.*, **90** (2003) 188301.
[8] Xinhui Lu, Mochrie S. G. J., Narayanan S., Sandy A. R. and Sprung M., *Phys. Rev. Lett.*, **100** (2008) 045701.
[9] Berne B. J. and Pecora R., *Dynamic Light Scattering: With Applications to Chemistry, Biology, and Physics* (John Wiley) 1976.
[10] Williams G. and Watts D. C., *Trans. Faraday Soc.*, **66** (1970) 80.
[11] Cipelletti L. and Weitz D. A., *Rev. Sci. Instrum.*, **70** (1999) 3214.
[12] Grubel G., Madsen A. and Robert A., *X-Ray Photon Correlation Spectroscopy (XPCS)*, in *Soft-Matter Characterization*, 1st edition (Springer, New York, USA) 2008, pp. 953–995.
[13] `http://www.esrf.eu/UsersAndScience/Experiments/CBS/ID10`.
[14] `http://www.esrf.eu/Instrumentation/DetectorsAndElectronics/maxipix`.
[15] Poon W. C. K., Weeks E. R. and Royall C. P., *Soft Matter*, **8** (2012) 21.
[16] Pedersen J. S., *Adv. Colloid Interface Sci.*, **70** (1997) 171.
[17] Aragón S. R. and Pecora R., *J. Chem. Phys.*, **64** (1976) 2395.
[18] Hansen J. P. and McDonald I. R., *Theory of Simple Liquids*. 4th edition (Academic Press) 2013.
[19] Ornstein L. S. and Zernike F., *Proc. Acad. Sci. Amsterdam*, **17** (1914) 793.
[20] Verwey E. J. W. and Overbeek J. Th. G., *Theory of the Stability of Lyophobic Colloids* (Elsevier Publishing Company, New York) 1948.
[21] Derjaguin B. V. and Landau L., *Acta Phys. Chim. URSS*, **14** (1941) 633.
[22] Lebowitz J. L. and Percus J. K., *Phys. Rev.*, **144** (1966) 251.

[23] Hayter J. B. and Penfold J., *Mol. Phys.*, **42** (1981) 109.
[24] Moynihan C. T. and Gupta P. K., *J. Non-Cryst. Solids*, **29** (1978) 143.
[25] Carroll J. P. and Patterson G. D., *J. Chem. Phys.*, **82** (1985) 9.
[26] Cipelletti L., Manley S., Ball R. C. and Weitz D. A., *Phys. Rev. Lett.*, **84** (2000) 2275.
[27] Ruta B., Baldi G., Monaco G. and Chushkin Y., *J. Chem. Phys.*, **138** (2013) 054508.
[28] Bouzid M., Colombo J., Barbosa L. V. and Del Gado E., *Nat. Commun.*, **8** (2017) 15846.
[29] Chaudhuri P. and Berthier L, *Phys. Rev. E*, **95** (2017) 060601.